A geometrical crossover in excited states of two-electron quantum dots in a magnetic field

R.G. Nazmitdinov [1,2], N. S. Simonović [3], A. R. Plastino [4,5], and A. V. Chizhov [2]

[1] Departament de Física, Universitat de les Illes Balears, 07122 Palma de Mallorca, Spain
[2] BLTP, Joint Institute for Nuclear Research, 141980 Dubna, Russia
[3] Institute of Physics, University of Belgrade, 11001 Belgrade, Serbia
[4] Instituto Carlos I de Fisica Teorica y Computacional, Universidad de Granada, 18071 Granada, Spain
[5] National University La Plata, UNLP-CREG-CONICET, C.C. 727, La Plata 1900, Argentina

E-mail: rashid@theor.jinr.ru

Abstract. We use the entanglement measure to study the evolution of quantum correlations in two-electron axially-symmetric parabolic quantum dots under a perpendicular magnetic field. We found that the entanglement indicates on the shape transition in the density distribution of two electrons in the lowest state with zero angular momentum projection at the specific value of the applied magnetic field.

1. Introduction

Nowadays there is a growing interest in using quantum entanglement measures for study of quantum correlations in topologically ordered systems [1]. The analysis of these systems is a highly non-trivial task due to the absence of the order parameter. Particular examples are the integer and fractional quantum Hall liquids which cannot be understood in terms of the traditional description of phases based on symmetry breaking and local order parameters. The main stream of such an analysis is focused on many-particle one-dimensional systems (cf [2]). Recently, topological phases were studied in finite systems such as two-dimensional electrons at very high magnetic field (Laughlin states) [3] and weakly interacting two-dimensional rotating Bose-Einstein condensate [4]. There are attempts to find a relation between topological orders of different topological phases and quantum phase transitions, driven by quantum fluctuations at zero temperature in many-body systems (see a textbook [5]).

It is believed that various quantum phases could exist in quantum dots (QDs) at different strengths of the applied perpendicular magnetic field [6]. At small magnetic field strengths one observes the orbital momentum and spin oscillations of the ground state of a QD by increasing the field strength. At certain field range the oscillations disappear and electrons form a fully polarized state called the maximum density droplet. It is expected that a further increase of the magnetic field should lead to the formation of the Wigner molecule, a finite-size analogue of the Wigner crystallization of the homogeneous electron gas. A natural question arises: if QDs can be considered as a finite-size analogy of conventional condensed matter systems what are signatures of quantum phase transitions in QDs ?

To shed light on this question we will employ the entanglement and compare its evolution with the evolution of quantum spectra of QDs as a function of the magnetic field. Evidently, finite systems can only show precursors of the QPT behaviour. However, they are also important for the development of the concept. Two-electron QDs being realictic tractable nontrivial systems are, in particular, attractive because their eigenstates can be obtained very accurately, or in some cases, exactly (cf [7, 8]). Moreover, it was found that at certain values of the magnetic field quantum spectra of two-electron QDs become degenerate due to onset of the spherical symmetry [9, 10]. The goal objective of the present paper is to demonstrate that a quantum entanglement can be used to indicate this transition in a three-dimensional (3D) quantum dot under a magnetic field.

2. Basics

Our analysis is carried out by means of the numerical diagonalization of the Hamiltonian

$$H = \sum_{j=1}^{2} \left[\frac{1}{2m^*} \left(\mathbf{p}_j - \frac{e}{c} \mathbf{A}_j \right)^2 + U(\mathbf{r}_j) \right] + \frac{k}{|\mathbf{r}_1 - \mathbf{r}_2|} + H_{spin}. \tag{1}$$

Here $k = e^2/4\pi\varepsilon_0\varepsilon_r$ and $H_{spin} = g^*\mu_B(\mathbf{s}_1 + \mathbf{s}_2)\cdot\mathbf{B}$ describes the Zeeman term, where $\mu_B = e\hbar/2m_e c$ is the Bohr magneton. As an example, we will use the effective mass $m^* = 0.067m_e$, the relative dielectric constant $\varepsilon_r = 12$ and the effective Landé factor $g^* = -0.44$ (bulk GaAs values). For the perpendicular magnetic field we choose the vector potential with gauge $\mathbf{A} = \frac{1}{2}\mathbf{B}\times\mathbf{r} = \frac{1}{2}B(-y, x, 0)$. The confining potential is approximated by a 3D axially-symmetric harmonic oscillator $U(\mathbf{r}) = m^*[\omega_0^2\,(x^2+y^2) + \omega_z^2 z^2]/2$, where $\hbar\omega_z$ and $\hbar\omega_0$ are the energy scales of confinement in the z-direction and in the xy-plane, respectively.

By introducing the center of mass (CM) and relative coordinates: $\mathbf{R} = \frac{1}{2}(\mathbf{r}_1 + \mathbf{r}_2)$ and $\mathbf{r}_{12} = \mathbf{r}_1 - \mathbf{r}_2$, – the Hamiltonian (1), in agreement with the Kohn theorem [11], separates into the CM and relative-motion terms $H = H_{\rm CM} + H_{\rm rel}$ (see details in [8]). The CM term is described by the oscillator Hamiltonian with the mass $\mathcal{M} = 2m^*$ and frequencies of the one-particle confining potential U. The Hamiltonian for relative motion in cylindrical coordinates takes the form

$$H_{\rm rel} = \frac{1}{2\mu}\Big(p_{\rho_{12}}^2 + \frac{l_z^2}{\rho_{12}^2} + p_{z_{12}}^2\Big) + \frac{\mu}{2}(\Omega^2\rho_{12}^2 + \omega_z^2 z_{12}^2) + \frac{k}{r_{12}} - \omega_L l_z, \tag{2}$$

where $\mu = m^*/2$ is the reduced mass, l_z ($\rightarrow -i\hbar\partial/\partial\varphi_{12}$) is the projection of angular momentum for relative motion and $\rho_{12} = (x_{12}^2 + y_{12}^2)^{1/2}$, $\varphi_{12} = \arctan(y_{12}/x_{12})$, $r_{12} = (\rho_{12}^2 + z_{12}^2)^{1/2}$. Here, $\omega_L = eB/2m^*c$ is the Larmor frequency, and the effective lateral confinement frequency $\Omega = (\omega_L^2 + \omega_0^2)^{1/2}$ depends through ω_L on the magnetic field.

The total two-electron wave function $\Psi(\mathbf{r}_1, \mathbf{r}_2) = \psi(\mathbf{r}_1, \mathbf{r}_2)\chi(\sigma_1, \sigma_2)$ is a product of the orbital $\psi(\mathbf{r}_1, \mathbf{r}_2)$ and spin $\chi(\sigma_1, \sigma_2)$ wave functions. Due to the Kohn theorem, the orbital wave function is factorized as a product of the CM and the relative motion wave functions

$$\psi(\mathbf{r}_1, \mathbf{r}_2) = \psi_{\rm CM}(\mathbf{R})\,\psi_{\rm rel}(\mathbf{r}_{12}). \tag{3}$$

According to the Pauli principle, the orbital wave function must be symmetric (or, equivalently, $\psi_{\rm rel}(\mathbf{r}_{12})$ must be even) for the antisymmetric (singlet: $S = M_S = 0$) spin state, and it must be antisymmetric ($\psi_{\rm rel}(\mathbf{r}_{12})$ must be odd) for the symmetric (triplet: $S = 1$, $M_S = 0, \pm 1$) spin states. Thus, for the relative motion the parity of $\psi_{\rm rel}(\mathbf{r}_{12})$ is a good quantum number as well as the magnetic quantum number m, since l_z is the integral of motion.

The CM eigenfunction is a product of the Fock-Darwin state (the eigenstate of electron in an isotropic 2D harmonic oscillator potential under a perpendicular magnetic field) [12]

in the (X,Y)-plane and the oscillator function in the Z-direction (both sets for a particle of mass $\mathcal{M}$). In this paper we consider the lowest CM eigenstate which has the form $\psi_{\rm CM}(\mathbf{R}) = \psi^{(xy)}_{\rm CM}(X,Y)\,\psi^{(z)}_{\rm CM}(Z)$, where $\psi^{(xy)}_{\rm CM}(X,Y) = \sqrt{2\bar{\Omega}/\pi}\,e^{-\bar{\Omega}(X^2+Y^2)}$ and $\psi^{(z)}_{\rm CM}(Z) = (2\bar{\omega}_z/\pi)^{1/4}e^{-\bar{\omega}_z Z^2}$ (i.e. zero principle quantum numbers), with $\bar{\Omega} = m^*\Omega/\hbar$ and $\bar{\omega}_z = m^*\omega_z/\hbar$.

Since the Coulomb interaction mixes the eigenstates of non-interacting electrons, the eigenfunctions of the Hamiltonian for relative motion (2) are expanded in the basis of the Fock-Darwin states $\Phi_{n,m}(\rho_{12},\varphi_{12})$ and oscillator functions in the z_{12}-direction $\phi_{n_z}(z_{12})$ (for a particle of mass μ), i.e.

$$\psi_{\rm rel}(\mathbf{r}_{12}) = \sum_{n,n_z} c^{(m)}_{n,n_z}\,\Phi_{n,m}(\rho_{12},\varphi_{12})\,\phi_{n_z}(z_{12}). \tag{4}$$

The coefficients $c^{(m)}_{n,n_z}$ can be determined by diagonalizing the Hamiltonian (2) in the same basis. Evidently, in numerical analysis the basis is restricted to a finite set $\{\Phi_{n,m}\,\phi_{n_z}|\,n = 0,\ldots,n_{\rm max};\ n_z = 0,\ldots,n_z^{\rm max}\}$. It must be, however, large enough to provide a good convergence for the numerical results. Since the function $\psi_{\rm rel}(\mathbf{r}_{12})$ has a definite parity and the parity of the functions $\Phi_{n,m}\,\phi_{n_z}$ is $(-1)^{m+n_z}$, the index n_z in the expansion (4) takes either even or odd values.

For non-interacting electrons ($k = 0$) the eigenfunctions $\psi_{\rm rel}$ are simply the basis functions $\Phi_{n,m}\,\phi_{n_z}$, and, therefore, the ground state is described by the wave function $\psi_{\rm rel} = \Phi_{0,0}\,\phi_0$. When two interacting electron move in the external field created by the confining potential and the applied, varying steadily, magnetic field, the quantum number m of the ground state (in the form (4)) evolves from zero to higher values as the magnetic field strength increases. It results in the well known singlet-triplet transitions [13]. Namely, for a given m the dominant term in the expansion (4) will be $\Phi_{0,m}\,\phi_0$ ($\Rightarrow$ all n_z are even) and the parity of the ground state is $(-1)^m$, which determines the total spin to be $S = \frac{1}{2}[1-(-1)^m]$. Note that the quantum number M_S associated with the spin wave function evolves as following: for even m the total spin $S = 0$ and, thus, $M_S = 0$; for odd m the total spin $S = 1$ and M_S can be -1, 0 or 1. The Zeeman splitting (with $g^* < 0$) will lower the energy of the $M_S = 1$ component of the triplet states, while leaving the singlet states unchanged. As a consequence, the ground state will be characterized by $M_S = S$. With the increasing magnetic field the intervals of the triplet states will increase at the cost of the singlet ones, and eventually, the singlet ground states will be totally suppressed. The increase of the magnetic field leads to the formation of a ring and a torus of maximal density in 2D- and 3D-densities, respectively (see Fig. 4 in Ref.[14]).

At the value $\omega_L^{\rm sph} = (\omega_z^2 - \omega_0^2)^{1/2}$ the magnetic field gives rise to the *spherical symmetry* ($\omega_z/\Omega = 1$) (with $\omega_z > \omega_0$) in the *axially-symmetric* two-electron QD [9, 10]. This phenomenon was also recognized in the results for many interacting electrons in self-assembled QDs [15]. In the later case it was interpreted as an approximate symmetry that had survived from the non-interacting case due to the dominance of the confinement energy over a relatively small Coulomb interaction energy. However, the symmetry is not approximate but *exact* even for strongly interacting electrons, because the radial electron-electron repulsion does not break the rotational symmetry. A natural question arises how to detect such a transition looking on the density distribution only. The related question is, if such a transition occurs, what are the concomitant structural changes?

To this end we employ the entanglement measure based on the linear entropy of reduced density matrices (cf [16])

$$\mathcal{E} = 1 - 2\,{\rm Tr}[{\rho_r^{(orb)}}^2]\,{\rm Tr}[{\rho_r^{(spin)}}^2], \tag{5}$$

where $\rho_r^{(orb)}$ and $\rho_r^{(spin)}$ are the single-particle reduced density matrices in the orbital and spin spaces, respectively. This measure is quite popular for the analysis of the entanglement of two-

fermion systems, in particular, two electrons confined in the parabolic potential in the absence of the magnetic field [17].

The trace $\mathrm{Tr}[{\rho_r^{(spin)}}^2]$ of the two-electron spin states with a definite symmetry χ_{S,M_S} has two values: (i) 1/2 if $M_S = 0$ (anti-parallel spins of two electrons); (ii) 1 if $M_S = \pm 1$ (parallel spins). The condition $M_S = S = \frac{1}{2}[1 - (-1)^m]$ yields

$$\mathrm{Tr}[{\rho_r^{(spin)}}^2] = \tfrac{1}{2}(1 + |M_S|) = \frac{3 - (-1)^m}{4}. \tag{6}$$

The trace of the orbital part $\mathrm{Tr}[{\rho_r^{(orb)}}^2]$

$$\begin{aligned}\mathrm{Tr}[{\rho_r^{(orb)}}^2] \;=\; \int d\mathbf{r}_1\, d\mathbf{r}_1{}'\, d\mathbf{r}_2\, d\mathbf{r}_2{}'\, \psi(\mathbf{r}_1,\mathbf{r}_2)\, \psi^*(\mathbf{r}_1{}',\mathbf{r}_2) \\ \psi^*(\mathbf{r}_1,\mathbf{r}_2{}')\, \psi(\mathbf{r}_1{}',\mathbf{r}_2{}').\end{aligned} \tag{7}$$

is more involved. Indeed, in virtue of Eqs.(3), (4), one obtains

$$\begin{aligned}\mathrm{Tr}[{\rho_r^{(orb)}}^2] = \sum_{n_1=0}^{n_{\max}}\sum_{n_2=0}^{n_{\max}}\sum_{n_3=0}^{n_{\max}}\sum_{n_4=0}^{n_{\max}}\sum_{n_{z_1}=0}^{n_z^{\max}}\sum_{n_{z_2}=0}^{n_z^{\max}}\sum_{n_{z_3}=0}^{n_z^{\max}}\sum_{n_{z_4}=0}^{n_z^{\max}} \\ c^{(m)}_{n_1,n_{z_1}} c^{(m)}_{n_2,n_{z_2}} c^{(m)}_{n_3,n_{z_3}} c^{(m)}_{n_4,n_{z_4}} \\ I(n_1,n_2,n_3,n_4;m)\, J(n_{z_1},n_{z_2},n_{z_3},n_{z_4}),\end{aligned} \tag{8}$$

where

$$\begin{aligned}I(n_1,n_2,n_3,n_4;m) = \int d\mathbf{r}_1\, d\mathbf{r}_1{}'\, d\mathbf{r}_2\, d\mathbf{r}_2{}' \\ \psi^{(xy)}_{\mathrm{CM}}(\tfrac{\mathbf{r}_1+\mathbf{r}_2}{2})\, \psi^{(xy)^*}_{\mathrm{CM}}(\tfrac{\mathbf{r}_1{}'+\mathbf{r}_2}{2})\, \psi^{(xy)^*}_{\mathrm{CM}}(\tfrac{\mathbf{r}_1+\mathbf{r}_2{}'}{2})\, \psi_{\mathrm{CM}}(\tfrac{\mathbf{r}_1{}'+\mathbf{r}_2{}'}{2}) \\ \Phi_{n_1,m}(\mathbf{r}_1-\mathbf{r}_2)\, \Phi^*_{n_2,m}(\mathbf{r}_1{}'-\mathbf{r}_2)\, \Phi^*_{n_3,m}(\mathbf{r}_1-\mathbf{r}_2{}')\, \Phi_{n_4,m}(\mathbf{r}_1{}'-\mathbf{r}_2{}')\end{aligned} \tag{9}$$

(here $\mathbf{r}_i$ are vectors in the xy-plane) and

$$\begin{aligned}J(n_{z_1},n_{z_2},n_{z_3},n_{z_4}) = \int dz_1\, dz_1{}'\, dz_2\, dz_2{}' \\ \psi^{(z)}_{\mathrm{CM}}(\tfrac{z_1+z_2}{2})\, \psi^{(z)^*}_{\mathrm{CM}}(\tfrac{z_1{}'+z_2}{2})\, \psi^{(z)^*}_{\mathrm{CM}}(\tfrac{z_1+z_2{}'}{2})\, \psi^{(z)}_{\mathrm{CM}}(\tfrac{z_1{}'+z_2{}'}{2}) \\ \phi_{n_{z_1}}(z_1-z_2)\, \phi^*_{n_{z_2}}(z_1{}'-z_2)\, \phi^*_{n_{z_3}}(z_1-z_2{}')\, \phi_{n_{z_4}}(z_1{}'-z_2{}').\end{aligned} \tag{10}$$

The magnetic field dependence of the entanglement $\mathcal{E}$ naturally occurs via inherent variability of the expansion coefficients. The values of the I and J integrals for any choice of indices can be determined analytically, which simplifies the numerical calculations.

For our analysis it is convenient to use the so-called Wigner parameter $R_W = (k/l_0)/\hbar\omega_0 = l_0/a^*$, a measure of the Coulomb interaction strength relative to the confinement strength (cf [8]). Here, $l_0 = \sqrt{\hbar/m^*\omega_0}$ is the oscillator length and $a^* = \hbar^2/km^*$ is the effective Bohr radius. For our choice of the parameters (GaAs) and for the confinement frequency $\hbar\omega_0 \approx 2.8$ meV we have $R_W \approx 2$. The numerical analysis demonstrates a good convergency for the basis with $n_{max} = n_z^{max} = 4$.

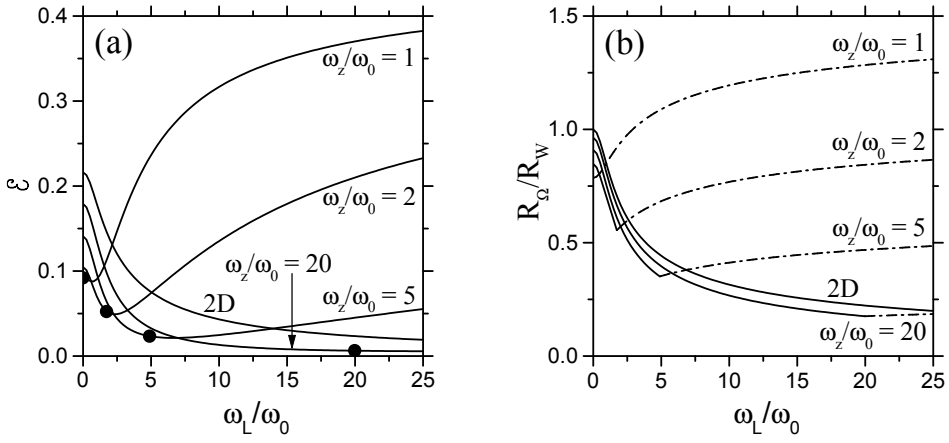

Figure 1. (a) Entanglement of the lowest state with $m = 0$ at $R_W = 2$ and various ratios ω_z/ω_0 as functions of the parameter ω_L/ω_0. The circles denote the values of ω_L/ω_0 when QDs with given ratios ω_z/ω_0 become spherically symmetric. (b) The relative strength of the Coulomb interaction $R_\Omega^{(2D)}/R_W$ (solid line) and $R_\Omega^{(1D)}/R_W$ (dash-dotted line) for the lowest state with $m = 0$ at various ratios ω_z/ω_0 as functions of the parameter ω_L/ω_0.

3. Analysis of results

The strongest correlations are expected for the states with $m = 0$, since they are not affected by the orbital electron motion which weakens the Coulomb interaction. In the absence of the magnetic field ($B = 0$) the entanglement decreases if the ratio ω_z/ω_0 decreases from ∞ (2D model) to 1 (spherically symmetric 3D model); see Fig. 1(a) at $\omega_L/\omega_0 = 0$. This effect could be explained by introducing the effective charge $k_{\rm eff}$ [9, 18] which determines the effective electron-electron interaction $V_C = k_{\rm eff}/\rho_{12}$ in the QD. In the 3D dot the electrons can avoid each other more effectively than in the 2D one. Therefore, the Coulomb interaction has a smaller effect on the 3D spectrum (the ratio $k_{\rm eff}/k \sim 0.5$) in contrast to the 2D case when $k_{\rm eff}/k = 1$. Thus, a decreasing of the ratio ω_z/ω_0 yields an analogous effect as the reduction of the electron-electron interaction.

Fig. 1(a) shows the entanglement measure $\mathcal{E}$ of the lowest angular momentum state $m = 0$ as a function of the magnetic field (the parameter ω_L/ω_0) at a fixed value of R_W and for different ratios ω_z/ω_0. In the 2D case the entanglement decreases monotonically with the increase of the magnetic field. The constant electron-electron interaction becomes relatively weaker, since the effective lateral confinement ($\hbar\Omega$) increases with the magnetic field. If we introduce the characteristic length of the effective confinement $l_\Omega = \sqrt{\hbar/m^*\Omega}$, the parameter $R_\Omega = l_\Omega/a^*$ (which is equal R_W at $B = 0$) determines the relative strength of Coulomb interaction at a given effective confinement. Evidently, R_Ω decreases with the increase of the magnetic field B (see Fig. 1(b), the line labelled by '2D'). In the 3D case, however, the entanglement decreases until $\omega_L = \omega_L^{\rm sph}$, when the spherical symmetry occurs. After this point the entanglement starts to increase (see Fig. 1(a)).

This behaviour can be explained by the influence of magnetic field on the effective strength R_Ω, which is twofold here. Indeed, in the 3D case the magnetic field affects the effective charge as well as the effective confinement. For the quasi-2D system of electrons ($\Omega \ll \omega_z$) the effective charge is $k_{\rm eff}^{(2D)} = \langle \rho_{12} V_C \rangle$ (see Eq. (18) in Ref. [18]), where $V_C = k/\sqrt{\rho_{12}^2 + z_{12}^2}$ is the full 3D Coulomb interaction. The mean value $\langle \rho_{12} V_C \rangle$ is calculated by means of the eigenstates of $H_{\rm rel}$ in the approximation of non-interacting electrons. Here, the eigenstate is $\Phi_{0,m}\,\phi_0$ (for

explicit expressions see Eqs. (19),(20) in Ref. [18]). Thus, for the quasi-2D case the parameter $R_\Omega^{(2D)} = (m^*/\hbar^3\Omega)^{1/2}\, k_{\rm eff}^{(2D)}$ can be used as a measure for the relative strength of the Coulomb interaction.

For $\Omega \gg \omega_z$ (very strong magnetic field) the electrons are pushed laterally towards the dot's center. The magnetic field, however, does not affect the vertical confinement. As a consequence the electrons practically can move only in the z-direction and the QD becomes a quasi-1D system. In this case a measure for the relative strength of Coulomb interaction can be defined as $R_\Omega^{(1D)} = (m^*/\hbar^3\omega_z)^{1/2}\, k_{\rm eff}^{(1D)}$, where the effective charge for a quasi-1D system is $k_{\rm eff}^{(1D)} = \langle |z_{12}| V_C \rangle$. It can be shown that for the lowest state with $m = 0$ one obtains $k_{\rm eff}^{(1D)}/k = (1 + \sqrt{\omega_z/\Omega})^{-1}$.

The quantities $R_\Omega^{(2D)}$ and $R_\Omega^{(1D)}$ for the lowest state with $m = 0$, as functions of the parameter ω_L/ω_0 (in the domains $0 < \omega_L < \omega_L^{\rm sph}$ and $\omega_L > \omega_L^{\rm sph}$, respectively), are shown in Fig. 1(b) for different ratios ω_z/ω_0. One observes that the effective strength $R_\Omega^{(2D)}$ decreases with the increase of the magnetic field for different ratios ω_z/ω_0, similar to the 2D case. The oppositely ordered confinement $\Omega^{(1D)}$ (which is not defined for the 2D case) increases with ω_L and, therefore, the effective strength $R_\Omega^{(1D)}$ increases as well. In order to match $R_\Omega^{(1D)} = R_\Omega^{(2D)}$ at $\omega_L = \omega_L^{\rm sph}$ (i.e. when $\Omega = \omega_z$) the strength $R_\Omega^{(1D)}$ is scaled by the factor $\pi/2$. Although at this point the 3D system is far from the 2D model and from the 1D model and, as a consequence, $R_\Omega^{(2D)}$ and $R_\Omega^{(1D)}$ do not match smoothly, these two functions taken together give a qualitative picture how the effective electron-electron interaction in a 3D QD changes with the magnetic field.

The minimum of entanglement for the lowest state with $m = 0$ at $\Omega = \omega_z$ can be associated with the condition of equivalence of the oscillator scales in the lateral and vertical confinements: $l_\Omega \equiv l_z = \sqrt{\hbar/m^*\omega_z}$. These quantities can be understood as the amplitudes of electron oscillations in the ρ and z-directions, respectively, for single-particle states with $n_\rho = 0$ and $n_z = 0$ [18]. At this point the effective Coulomb interaction becomes isotropic, which results in the small mixing of single-particle states, in contrast to the 2D and 1D cases. This result can be readily extended for the infinite square well potential in the z-direction. In this case $l_z \approx d/2$; d is the thickness of semiconductor layer where the dot is created (see Fig.1 in Ref. [18])). Therefore, the minimum of entanglement is expected at $l_\Omega = d/2$ which defines the value of the magnetic field by means of the Larmor frequency $\omega_L = \sqrt{(4\hbar/m^*d^2)^2 - \omega_0^2}$.

To get deep insight into this transition we calculate the probability density $|\psi(\mathbf{r}_{12})|^2$ and potential surfaces for various values of the magnetic field (see Fig. 2). Since the symmetry is exact for any strength of the electron-electron interaction at the transition point, in order to illuminate the effect, we use $R_W = 10$. For the magnetic field $\omega_L < \omega_L^{\rm sph}$ the density maximum is located in the (x_{12}, y_{12})-plane ($z_{12} = 0$, see Fig. 2(a)). For $\omega_L > \omega_L^{\rm sph}$, however, there are two maxima located symmetrically along the z_{12}-axis ($\rho_{12} = 0$, see Fig. 2(c)). The analysis of the behaviour of the stationary point of the potential $V = \frac{1}{2}\mu(\Omega^2\rho_{12}^2 + \omega_z^2 z_{12}^2) + k/r_{12}$ as a function of the magnetic field provides the explanation. For $\omega_L < \omega_L^{\rm sph}$ ($\Omega < \omega_z$) the stationary point $\rho_{12} = \rho_0$, $z_{12} = 0$ is the minimum of the potential surface (see Fig. 2(d)). Here $\rho_0 = (k/\mu\Omega^2)^{1/3}$ [19]. By increasing the magnetic field over the value $B_{\rm sph}$ ($\Omega > \omega_z$) the stationary point transforms to the saddle point and two new minima appear, divided by a potential barrier (see Fig. 2(f)). In other words, for $m = 0$ a bifurcation of the stationary point located at $(\rho_0, 0)$ occurs at the value of magnetic field when $\omega_L = \omega_L^{\rm sph}$ (see Fig. 2(b,e)). In the domain $\Omega > \omega_z$, for $m = 0$, the minima are located at $z_{12} = \pm z_0$ in the z_{12}-axis ($\rho_{12} = 0$), where $z_0 = (k/\mu\omega_z^2)^{1/3}$. Similar behavior is observed for the states with $m \neq 0$. However, the effect is less prominent due to weakening of correlations by the orbital electron motion.

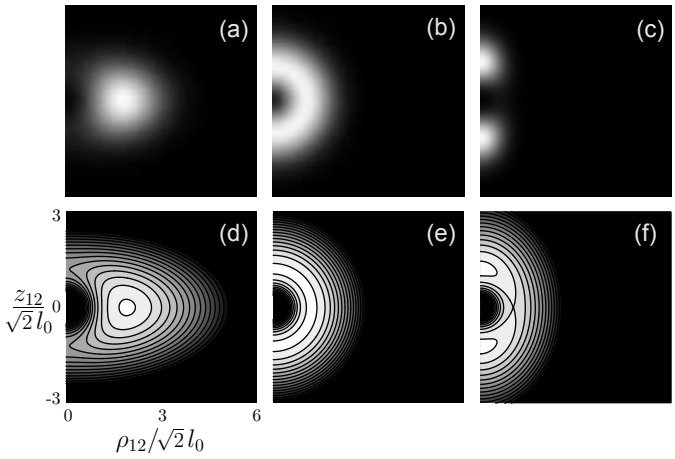

Figure 2. The probability density $|\psi(\mathbf{r}_{12})|^2$ of the lowest $m = 0$ state (top) and the contour plots of the potential surface (bottom) for the QD with $\omega_z/\omega_0 = 2$ and $R_W = 10$ shown in (ρ_{12}, z_{12})-plane for the cases: (a,d) $\omega_L/\omega_0 = 0$ $(\omega_z/\Omega = 2)$, (b,e) $\omega_L/\omega_0 = \omega_L^{\rm sph}/\omega_0 = 1.73205$ $(\omega_z/\Omega = 1)$ and (c,f) $\omega_L/\omega_0 = 2.29129$ $(\omega_z/\Omega = 0.8)$.

4. Conclusions

Summarizing, we have shown that the 3D approach provides a consistent description of the shape transition in the excited states of two-electron QDs under the magnetic field. The entanglement of the lowest state with $m = 0$, being first a decreasing function of the magnetic field, starts to increase after the transition point with the increase of the magnetic field. This behaviour is understood as the transition from the lateral to the vertical localization of the two-electron probability density for this state, which becomes prominent at strong Coulomb interaction $(R_W \gg 2)$.

Acknowledgments

This work is partly supported by RFBR Grant No.11-02-00086 (Russia), Project 171020 of Ministry of Education and Science of Serbia, Spanish MICINN Grant No. FIS2008-00781, and Project FQM-2445 of the Junta de Andalucia (Spain).

References

[1] Amico L, Fazio R, Osterloh A and Vedral V 2008 *Rev. Mod. Phys.* **80** 517
[2] Turner A M, Pollmann F and Berg E 2011 *Phys. Rev. B* **83** 075102; Fidkowski L and Kitaev A 2011 *Phys. Rev. B* **83** 075103
[3] Haque M, Zozulya O and Schoutens K 2007 *Phys. Rev. Lett.* **98** 060401
[4] Liu Z, Guo H-L, Vedral V and Fan H 2011 *Phys. Rev. A* **83** 013620
[5] Sachdev S *Quantum Phase Transitions* 2011 (Cambridge: Cambridge University Press) 2nd Edition
[6] Reimann S M and Manninen M 2002 *Rev. Mod. Phys.* **74** 1283
[7] Kais S, Herschbach D R and Levine R D 1989 *J. Chem. Phys.* **91** 7791; Taut M 1994 *J. Phys. A* **27** 1045
[8] Nazmitdinov R G 2009 *Physics of Particles and Nuclei* **40** 71
[9] Nazmitdinov R G, Simonović N S and Rost J M 2002 *Phys. Rev. B* **65** 155307
[10] Simonović N S and Nazmitdinov R G 2003 *Phys. Rev. B* **67** 041305(R)
[11] Kohn W 1961 *Phys. Rev.* **123** 1242
[12] Fock V 1928 *Z. Phys.* **47** 446; Darwin C G 1930 *Proc. Cambridge Philos. Soc.* **27** 86
[13] Wagner M, Merkt U and Chaplik A V 1992 *Phys. Rev. B* **45** 1951
[14] Nazmitdinov R G and Simonović N S 2007 *Phys. Rev. B* **76** 193306
[15] Wojs A, Hawrylak P, Fafard S and Jacak L 1996 *Phys. Rev. B* **54** 5604
[16] Coleman A and Yukalov V 2000 *Reduced Density Matrices* (Berlin: Springer-Verlag)

[17] Buscemi F, Bordone P and Bertoni A 2007 *Phys. Rev. A* **75** 032301; Naudts J and Verhulst T 2007 *Phys. Rev. A* **75** 062104; Coe J P, Sudbery A and Amico I D' 2008 *Phys. Rev. B* **77** 205122; Pipek J and Nagy I 2009 *Phys. Rev. A* **79** 052501; Yañez R J, Plastino A R and Dehesa J S 2010 *Eur. Phys. J. D* **56** 141; Kościk P and Okopińska A 2010 *Phys. Lett. A* **374** 3841
[18] Simonović N S and Nazmitdinov R G 2008 *Phys. Rev. A* **78** 032115
[19] Puente A, Serra L and Nazmitdinov R G 2004 *Phys. Rev. B* **69** 125315